

Mechanosensitive Channels and Tarantula Toxin

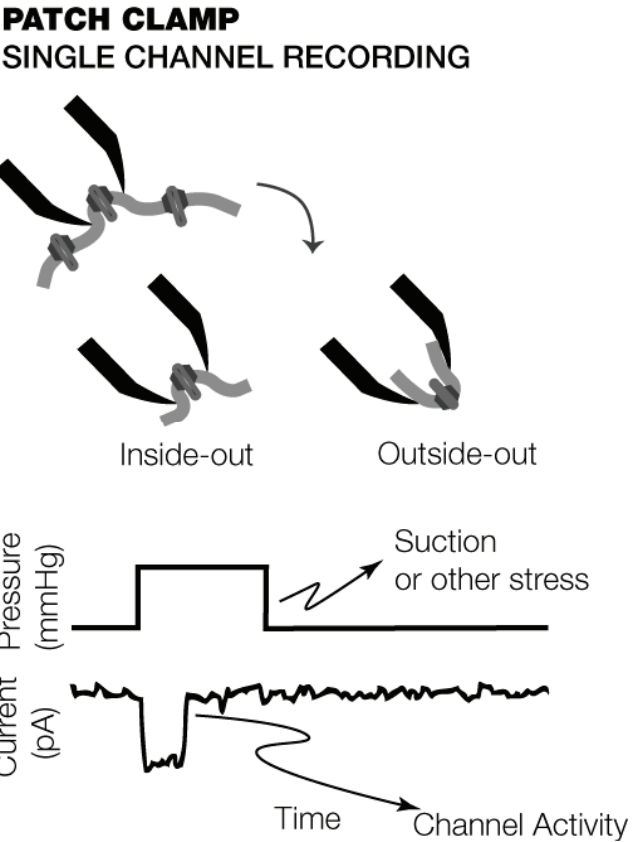
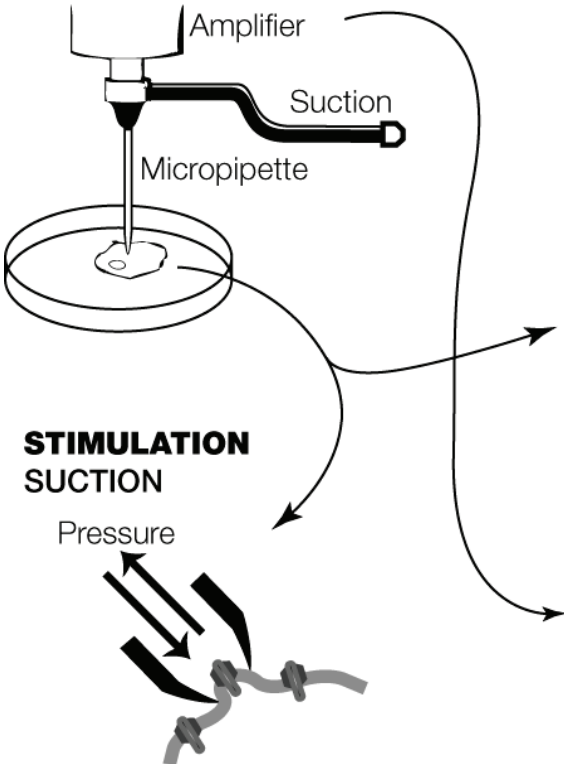
Ion channels can be functionally characterized on the basis of their gating properties: ligand binding can activate the channel, causing it to open (acetylcholine receptor is a classic example, other examples include inositol tris phosphate, ryanodine, neurotransmitter-gated channels etc.). Voltage gating is also very important, underlying the dynamics of an action potential. In addition, many channels are gated mechanically. The latter channel types are often called stretch-activated, because their original discovery was based on the observation of channel activation when applying suction to a patch of membrane in the patch clamp technique. But in fact, the gating may also involve mechanical stress on the cytoskeleton and special tethers in the case of channels in auditory systems (hearing).

After their original discovery in the 1980's, there was much controversy over the role of stretch-activated channels because of a discrepancy that was discovered relatively quickly: Although the channels could be observed in isolated patches of membrane, when whole cells were 'expanded' by increasing pressure in a whole cell patch clamp mode, there was no indication of a current activation consistent with a stretch-activated channel.

Nevertheless, over time, it became clear that mechanosensitive channels were not an artefact, and a variety of mechanisms for stretching the membrane did indeed result in the appearance of currents consistent with a functional stretch activated channel.

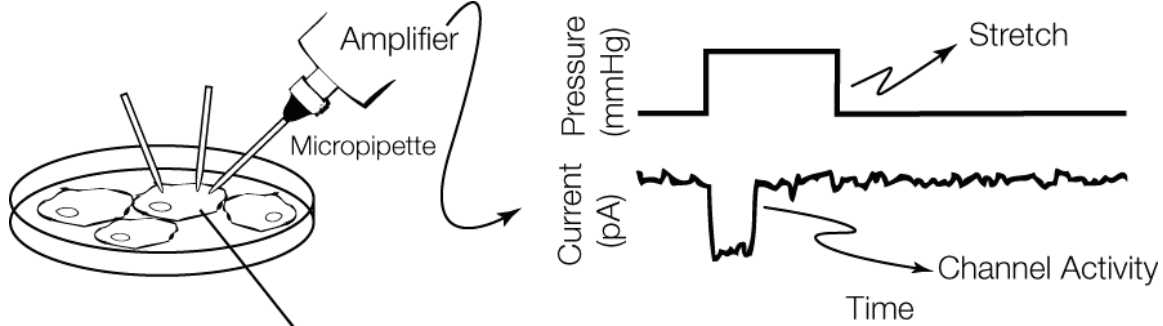
The next step was to clone the channels. This was by no means an easy task. The best characterized system is a mechanosensitive channel in *E. coli*. In the case of *E. coli*, the physiological role of the channel is apparently protecting the cell from lysis under hypotonic (hypoosmotic) conditions. When there is an osmotic imbalance between the intracellular and extracellular milieu, a pressure is created due to water flow. This is really an analog of the effect of differences in ion concentration that result in the creation of a voltage potential between the inside and outside of the cell.

Mechanical Stress by Suction



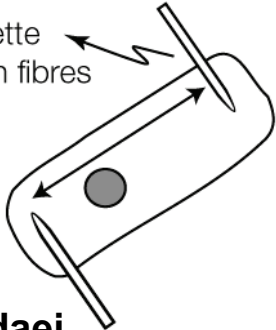
Nima Mirmoghtadaei
FALL 06 HONOURS THESIS

Mechanical Stress by End-to-End Stretch



**STIMULATION
END-TO-END
STRETCH**

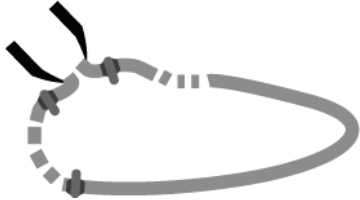
Micropipette
or Carbon fibres



**PATCH CLAMP
CELL ATTACHED**

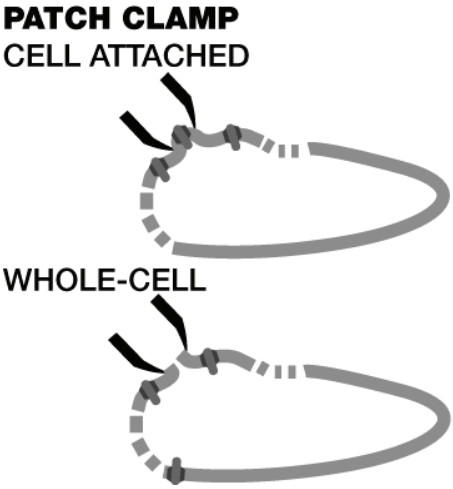
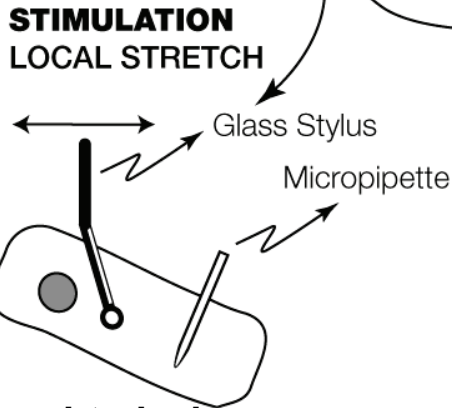
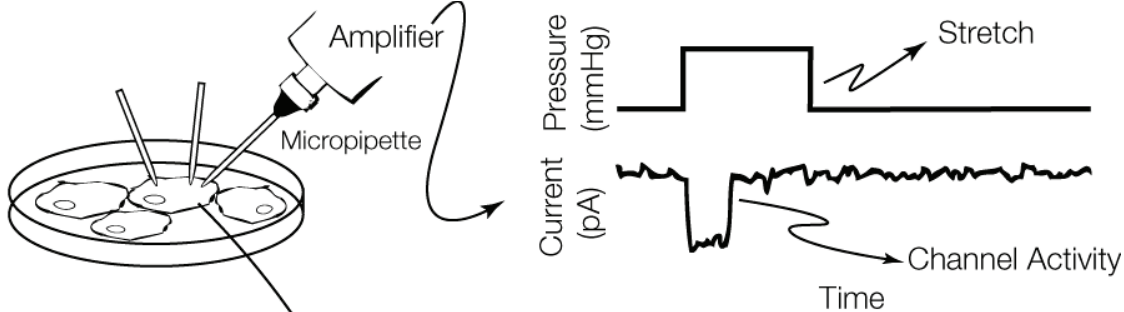


WHOLE-CELL



Nima Mirmoghtadaei
FALL 06 HONOURS THESIS

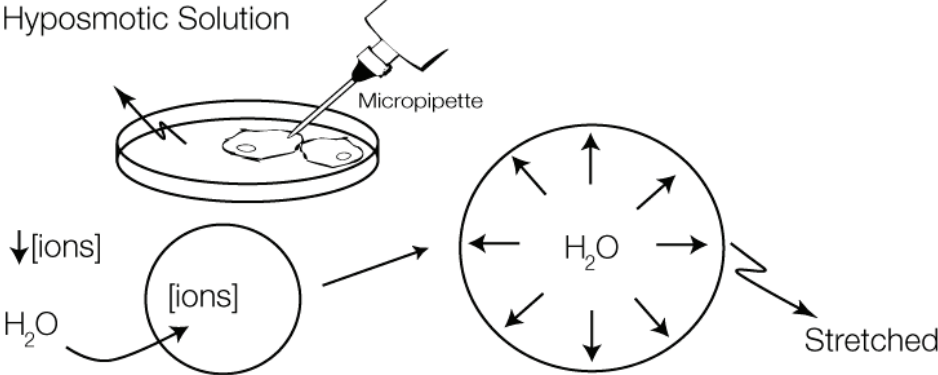
Mechanical Stress by Local Stretch



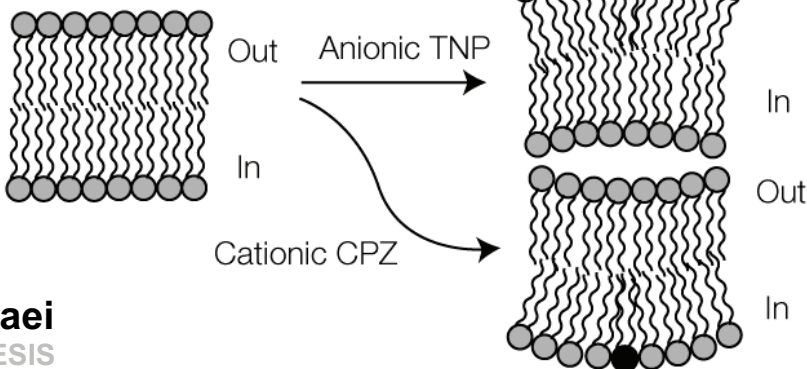
Nima Mirmoghtadaei
FALL 06 HONOURS THESIS

Mechanical Stress by Local Stretch

HYPOSMOTIC PRESSURE (OSMOTIC SWELLING)

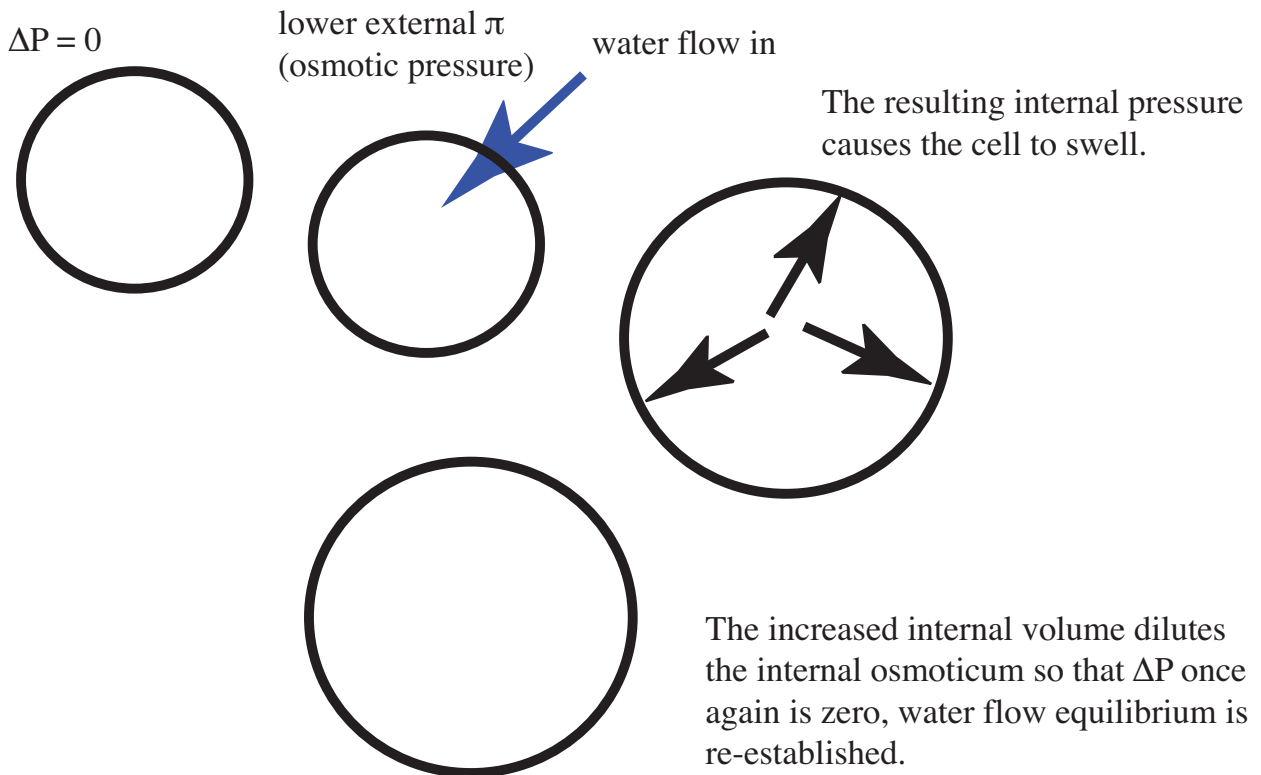
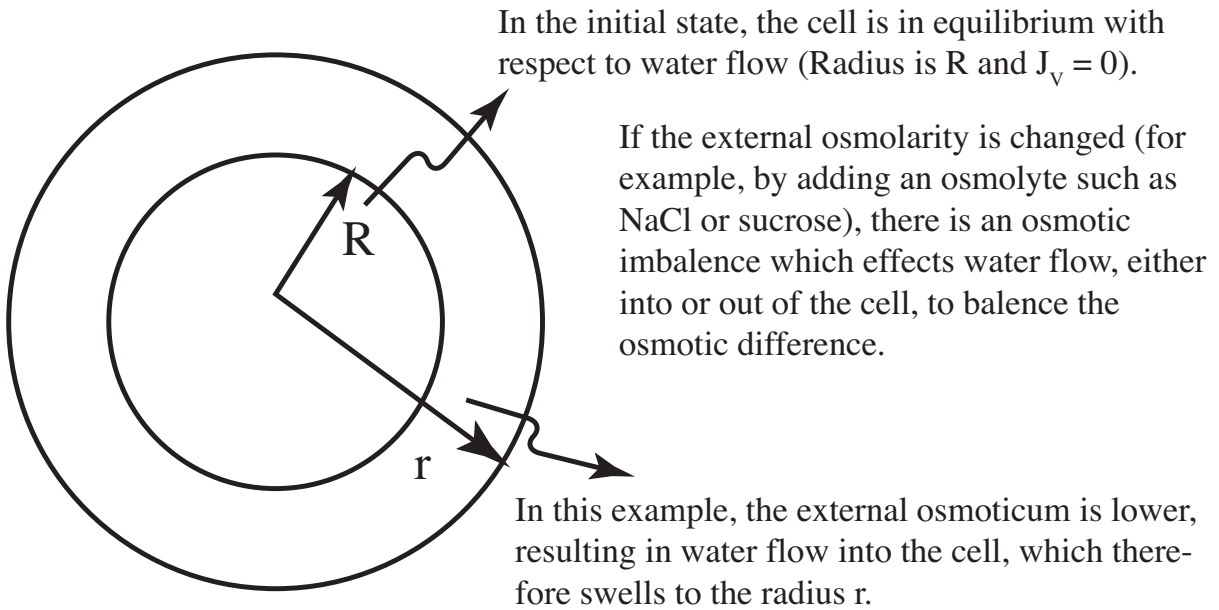


AMPHIPATHS

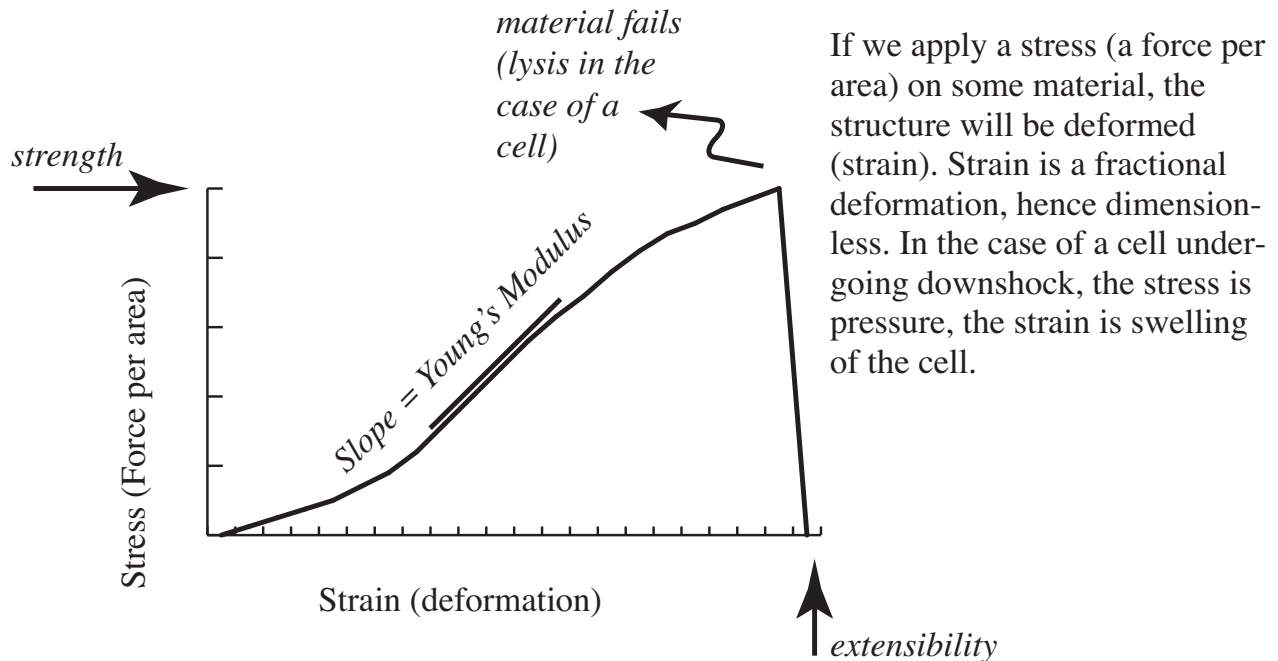


Nima Mirmoghtadaei
FALL 06 HONOURS THESIS

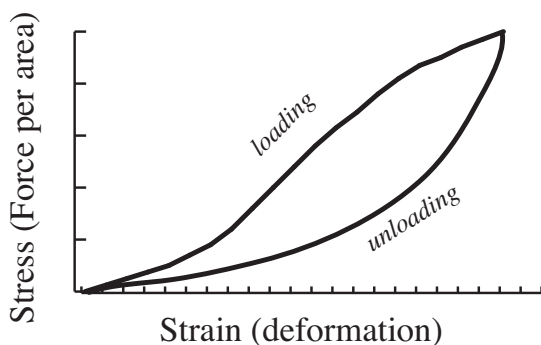
It is easiest to consider an isolated cell to consider how pressure and volume changes affect the well-being of the cell.



The extent of the cell swelling caused by lower external osmolarity (a *downshock*, in the parlance of volume regulation researchers) depends upon the nature of the outer cell wall of the cell. All cells have a wall, of some sort or another. It may be a glycocalyx, a polysaccharide coat, a chitin fibrillar network, a cellulosic framework or something else. Even silica can be used as an outer wall or coat. No matter the composition, it will resist the swelling caused by the pressure change. This is known as the modulus of elasticity.



The steeper the slope (the greater the value of Young's modulus, in units of force per area), the stiffer (less deformable) the material.



Experimentally, materials may be 'viscoelastic', leading to a stress-strain relation in which load and unloading of the force follow different paths of deformation.

^[1]Source: Vogel, Steven (1988) *Life's Devices. The physical world of animals and plants.* Princeton University Press. pp. 183–184.

The mathematical envelope underlying the changes in osmolarity, pressure and volume is complex, but exceedingly important for the survival of a cell (or organism for that matter)^[1].

Integration is required to determine P(t), V(t) and π(t)

$$J_V = -\frac{1}{A} \cdot \frac{dV}{dt} = L_p \cdot [P(t) + \pi^o + \Delta\pi^o - \pi^i(t)]$$

water flow
area
change in volume over time
hydraulic conductivity
change in pressure over time
the external osmotic pressure
the change in external osmotic pressure
the change in internal osmotic pressure over time

Note that in the absence of a change in external osmolarity, the equation has the form:

$$J_V = -\frac{1}{A} \cdot \frac{dV}{dt} = L_p \cdot [P - RT(c^i - c^o)] = L_p \cdot \Delta\Psi$$

where $RT(c^i - c^o) = \pi^i - \pi^o$

When the pressure and difference in osmotic pressure are equal: $P = RT(c^i - c^o)$
 Then the water flow is zero.

This is also true if the hydraulic conductivity (L_p) is zero or close enough to allow rapid change in cell volume.

^[1]Source: Zimmerman (1991) Pressure Probe Techniques. private publication.

The dependence of pressure on volume, $P(V)$, is described by the modulus of elasticity described earlier^[1]:

$$\frac{dP}{dV} = \frac{\varepsilon}{V} \approx \frac{\Delta P}{\Delta V} = \frac{P - P_0}{V - V_0}$$

elastic coefficient
of the cell

The dependence of internal osmotic potential ($RT \cdot c^i$) on volume, $\pi(V)$, can be described by^[1]:

$$\frac{d\pi^i}{dV} \approx \frac{\Delta\pi^i}{\Delta V} = \frac{\pi^i - \pi_0^i}{V - V_0}$$

osmotic potential and volume
at time zero.

Combining these results and integrating over the boundary conditions of P_0 at time zero and P_e at 'infinite' time:

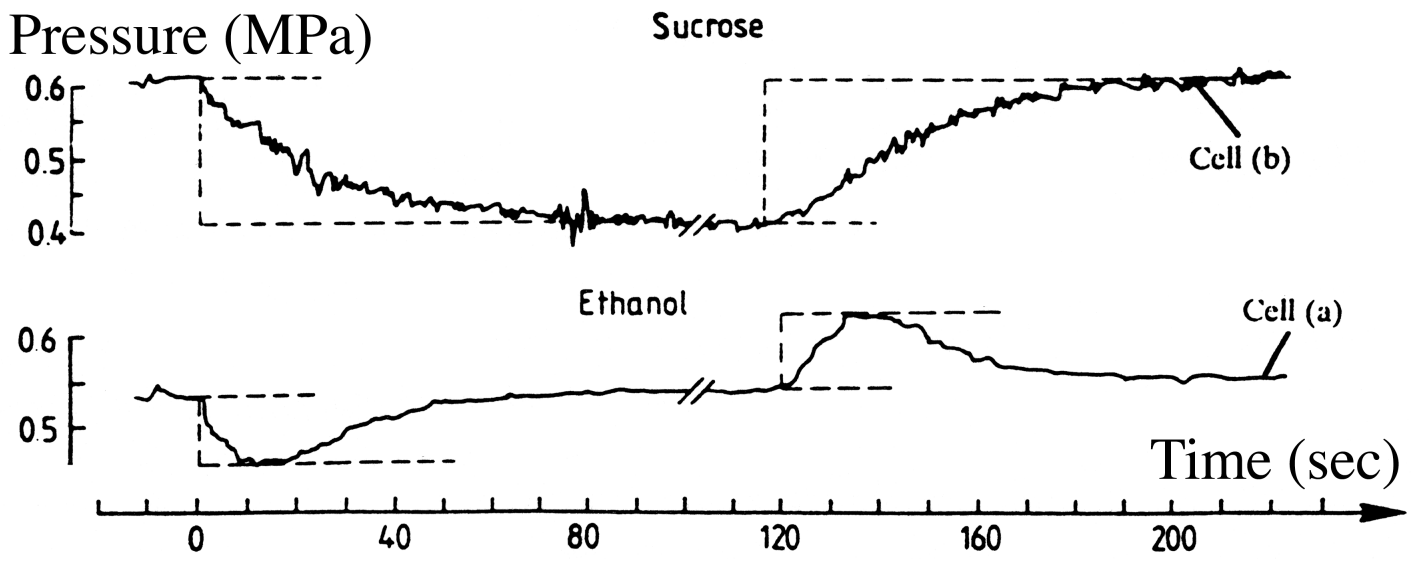
$$P_0 - P_e = \frac{\varepsilon}{\varepsilon + \pi_0^i} \cdot \Delta\pi^o$$

and $P(t)$:

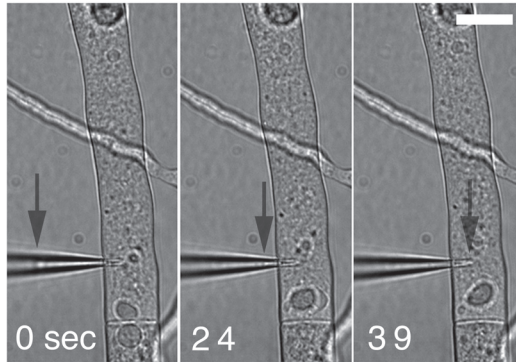
$$P(t) = (P_{initial} - P_e) \cdot e^{\left(-L_p \cdot A \cdot \frac{\varepsilon + \pi^i}{V} \cdot t\right)}$$

That is, an exponential change in pressure dependent on internal osmolarity, volume, cell area, and hydraulic conductivity.

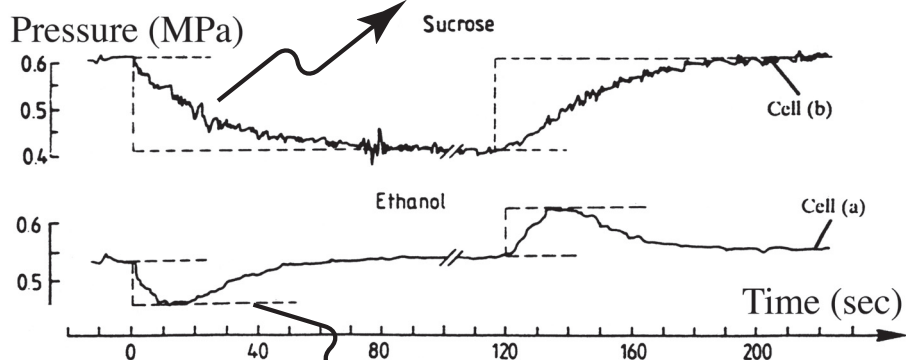
^[1]Source: Zimmerman (1991) Pressure Probe Techniques. private publication.



If the extracellular concentration of solutes is changed (either increased or decreased), water flow (either out of or into the cell) will cause a change in the hydrostatic pressure. This can be determined by maintaining the meniscus of the oil/water interface at the micropipette tip, and measuring the pressure required to do so. Two examples of such experiments are shown below. One in which the solute (osmolyte) added to the extracellular solution was sucrose; the other in which the added solute was ethanol^[1].



Sucrose addition causes the pressure to decrease. The time course reflects the time required for water to leave the cell.



Sucrose is apparently impermeant, while ethanol rapidly permeates. The time course, cell size, and concentration are all used to determine the permeability coefficients of the solutes.

Ethanol addition also causes the pressure to decrease, but the pressure returns to its original value: Because ethanol permeates the cell within the time frame of the experiment, re-equilibrating the solute concentrations.

Separate from the experimental determination of permeability coefficients, the phenomenon of osmotic pressure was originally explored by Pfeffer and others in plants (as well as model membrane systems) and created the knowledge base from which Einstein could elucidate the molecular mechanisms of the random walk from a thermodynamic perspective.

^[1]Anonymous (1993) Pressure Probe Techniques. Private Publication.

In bacteria, downshock (a dramatic decrease in extracellular osmolarity) causes water inflow, and thus a substantial increase in hydrostatic pressure that could burst the cell envelope.

A potential mechanism for ‘sensing’ downshock is mechanosensitive channels that would be activated by the stretching of the membrane as the cell volume increases (swelling). Using the patch clamp technique, mechanosensitive channels have been measured in bacteria. At least three channels have been identified as MscL (Large conductance, 3 nanoSiemen), MscM (Medium conductance, 1 nanoSiemen), and MscS (Small conductance, 0.3 nanoSiemen). The MscL was cloned and a null mutant created, which did not exhibit hypersensitivity to downshock, so the other channels, or some combination thereof, might be required, if indeed the channels function in downshock responses.

Levina et al. (1999)² analyzed sequences to identify putative candidate genes encoding the other mechanosensitive channels in *E. coli*, and discovered two putative channels: KefA and YggB. In the absence of both (that is, null mutants), *E. coli* had no MscS channel activity. The data is complex:

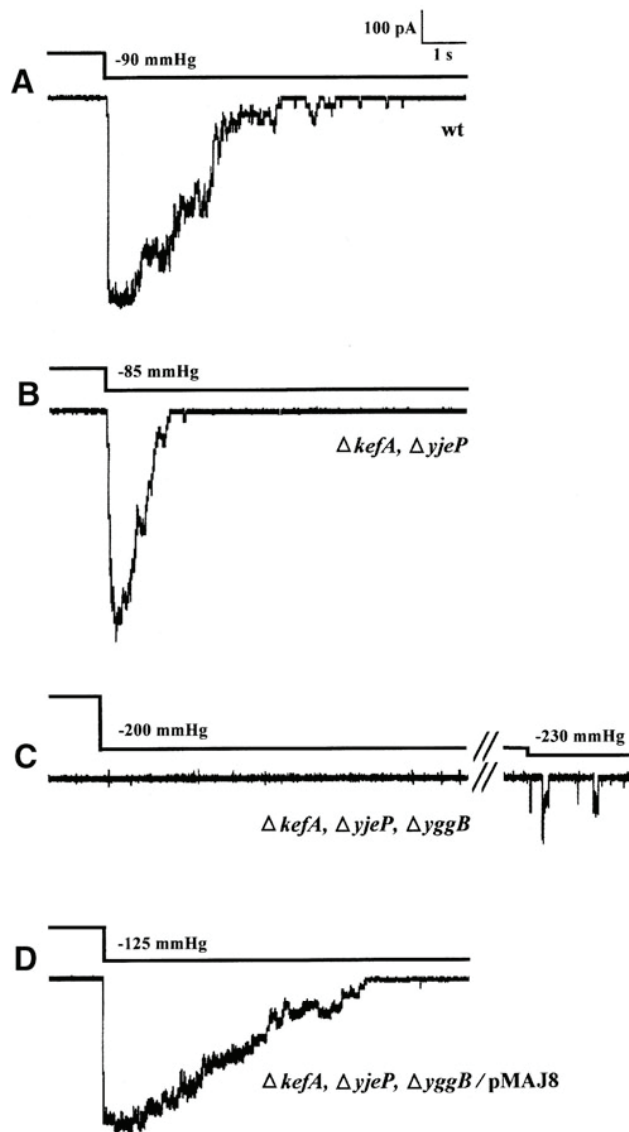
Δ yggB eliminates the major MscS activity, but reveals a similar channel activity that is less abundant, and does not ‘run-down’ (desensitize) with continued suction application.

Δ kefA removes the latter activity.

The next step was to examine the sensitivity of the bacteria to downshock, using a combinatorial approach in which the various null mutants were examined alone or in combination.

² Levina N, Töttemeyer S, Stokes NR, Louis P, Jones MA, Booth IR. (1999) Protection of *Escherichia coli* cells against extreme turgor by activation of MscS and MscL mechanosensitive channels: identification of genes required for MscS activity. *EMBO J.* 18:1730-1737.

YggB encodes the major MscS activity.

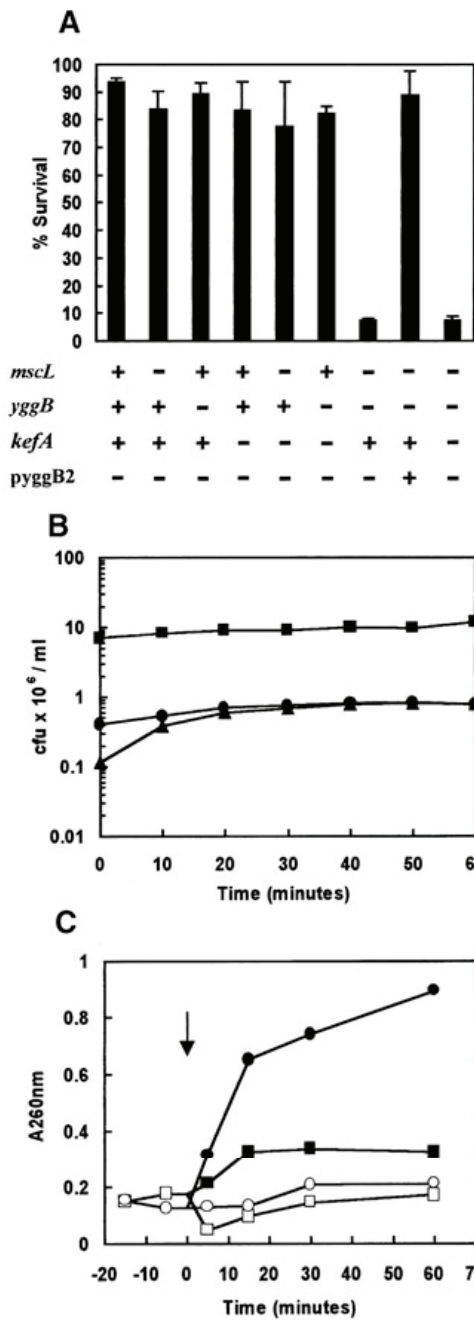


Patch-clamp recordings were made on (A) Frag1, (B) strain MJF421 (Frag1, $\Delta kefA$, $\Delta yjeP$), (C) strain MJF431 (Frag1, $\Delta kefA$, $\Delta yjeP$, $\Delta yggB$) and (D) MJF431/pMAJ8 as described in Materials and methods. In (C), the pressure was increased to confirm the presence of the MscL activity. The pressure on the patch is shown as a solid line immediately above the recording. The pressure required to activate the channels varies with patch geometry (Blount et al., 1996b) and there is no significance in the differences in pressure required to see MscS channel activity in individual experiments.

Levina N, Töttemeyer S, Stokes NR, Louis P, Jones MA, Booth IR. (1999) Protection of *Escherichia coli* cells against extreme turgor by activation of MscS and MscL mechanosensitive channels: identification of genes required for MscS activity. *EMBO J.* 18:1730-1737.

Survival of mechanosensitive channel mutants

upon downshock.



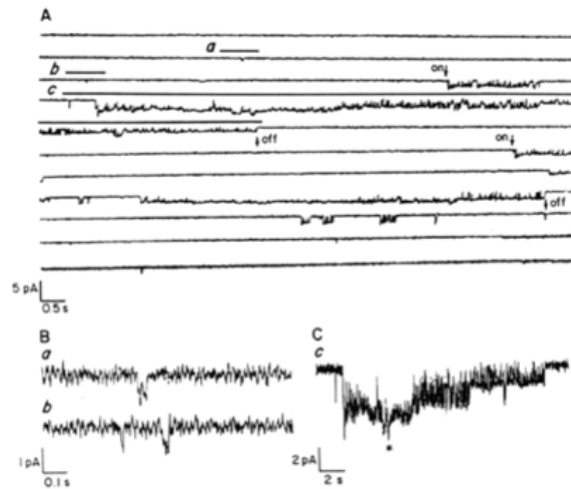
(A) Cells were grown to exponential phase in minimal medium (pH 7) in the presence of 0.5 M NaCl and diluted 20-fold into minimal medium without NaCl (pH 7). The data show the survival of the strains measured 30 min after a 0.5 M NaCl downshock. Survival after iso-osmotic dilution is set to 100% and no significant differences were observed under these conditions for any of the strains. Strains assayed: Frag1 (wild type); MJF367 ($\Delta mscL$); MJF451 ($\Delta yggB$); MJF379 ($\Delta kefA$); MJF453 ($\Delta kefA \Delta mscL$); MJF429 ($\Delta kefA, \Delta yggB$); MJF455 ($\Delta mscL \Delta yggB$); MJF455 ($\Delta mscL, \Delta yggB$)/*pyggB2*; MJF 465 ($\Delta kefA \Delta yggB \Delta mscL$). (B) Cells of strains Frag1 (filled square), MJF455 ($\Delta yggB, \Delta mscL$) (filled circle) and MJF465 ($\Delta yggB, \Delta mscL, \Delta kefA$) (filled triangle) were treated as in (A) and samples taken at timed intervals, and the apparent viability determined as described above. Data for iso-osmotic dilution are omitted for clarity and were found to be identical to the data for Frag1. (C) Cells were grown as described in (A), filtered and re-suspended in the presence (open symbols) or absence (closed symbols) of 0.5 M NaCl. At intervals, 3 ml samples were centrifuged and the OD₂₆₀ of the supernatant recorded. Symbols: (filled square, square) Frag1; (filled circle, circle) MJF455 ($\Delta mscL, \Delta yggB$). All of the data are representative of triplicate experiments and error bars display standard deviation from the mean for one experiment.

Levina N, Töttemeyer S, Stokes NR, Louis P, Jones MA, Booth IR. (1999) Protection of *Escherichia coli* cells against extreme turgor by activation of MscS and MscL mechanosensitive channels: identification of genes required for MscS activity. *EMBO J.* 18:1730-1737.

Hyphal organisms contain stretch-activated Ca^{2+} -permeant channels:

Gadolinium inhibits the stretch-activated Ca^{2+} channels.

Inhibiting the channels irreversibly in *Saprolegnia ferax*^[1], transiently in *Neurospora crassa*^[2].



Example of stretch-activated (SA) Ca^{2+} channel activity in *Saprolegnia ferax*^[3].

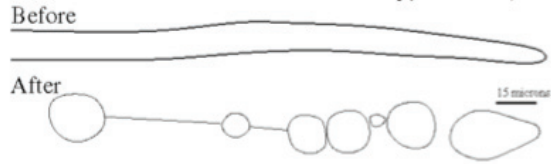
^[1] Garrill A, SL Jackson, RR Lew, IB Heath (1993) Ion channel activity and tip growth: tip-localized stretch-activated channels generate an essential Ca^{2+} gradient in the oomycete *Saprolegnia ferax*. *Eur. J. Cell Biol.* 60:358-365.

^[2] Lexina, NN, RR Lew, GJ Hyde, IB Heath (1995) The roles of calcium ions and plasma membrane ion channels in hyphal tip growth of *Neurospora crassa*. *J. Cell Sci.* 108:3405-3417.

^[3] Lexina, NN, RR Lew, IB Heath (1994) *J. Cell Sci.* 107:127-134.

Spatial Distribution of Ion Channels along the Hyphal Tip

Because spatial information was retained after wall digestion, it was possible to examine channel frequencies along the hypha:



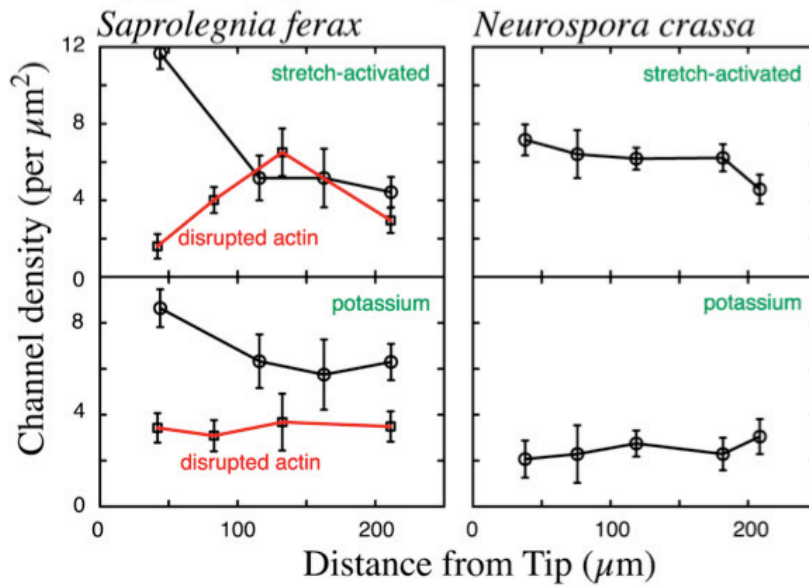
Channel Type and Observed Frequency^[1]

Protoplast Origin	K ⁺	SA	K ⁺ and SA	none
apical (n=36)	19	3	11	3
posterior (n=24)	11	0	2	11

Measuring channel densities was the next step.

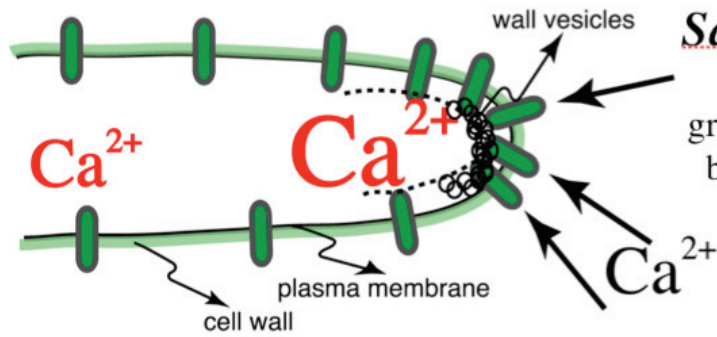
^[1] Garrill A, RR Lew, IB Heath (1992) Stretch-activated Ca²⁺ and Ca²⁺-activated K⁺ channels in the hyphal tip plasma membrane of the oomycete *Saprolegnia ferax*. *J. Cell Sci.* 101:721-730.

Differences in channel distributions (*S. ferax* had tip-high channel densities, *N. crassa* did not) suggested differences in the control of tip growth by ion transport.

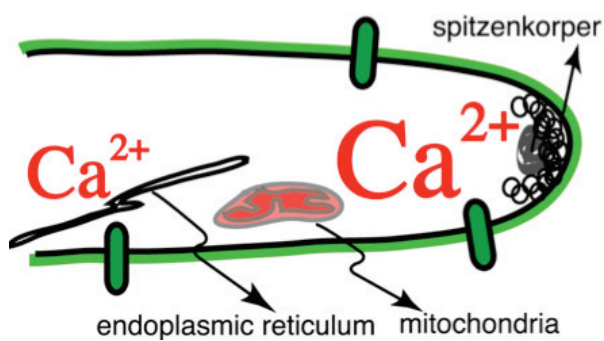


Ca²⁺ and K⁺ channel densities versus distance from the tip in *Saprolegnia ferax* and *Neurospora crassa*^[1].

^[1] Lew RR (1993) Mapping fungal ion channel distributions. Fungal Genet. Biol. 24: 69-76.

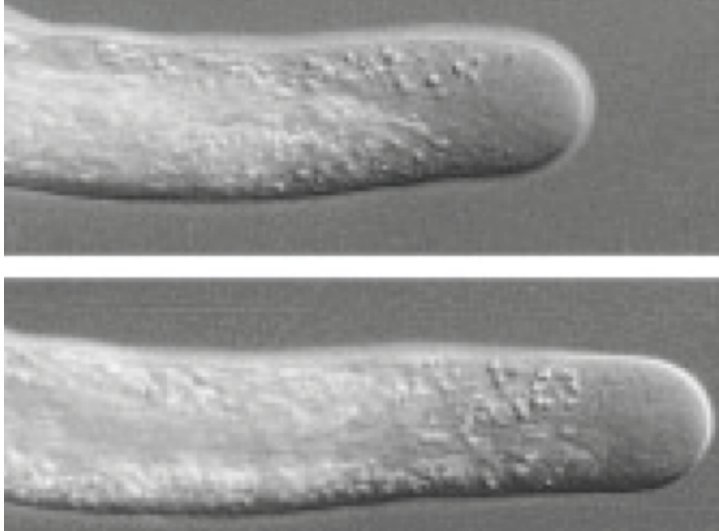


***Saprolegnia*:** Calcium influx is required for tip growth. Influx is mediated by the activity of stretch-activated calcium permeable channels.

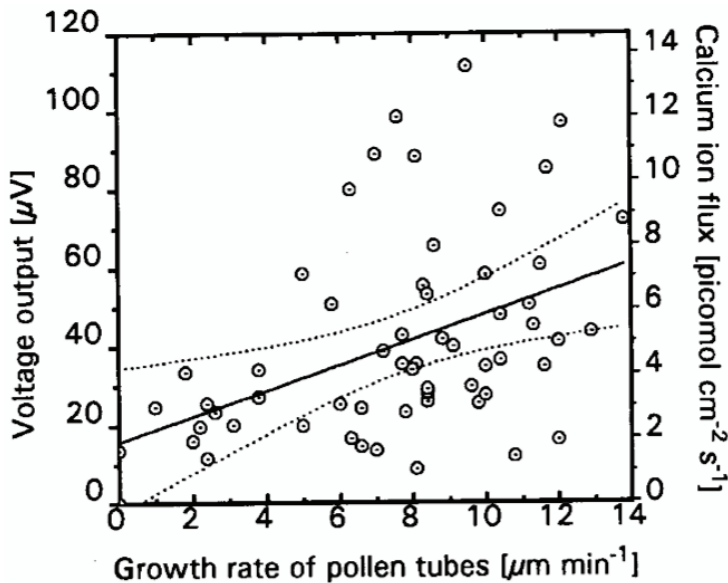


***Neurospora*:** Calcium influx does not occur during tip growth. However, a tip-high calcium gradient is required for tip growth, but must be generated internally.

Growing pollen tubes require an internal tip-high Ca^{2+} gradient for tip expansion.



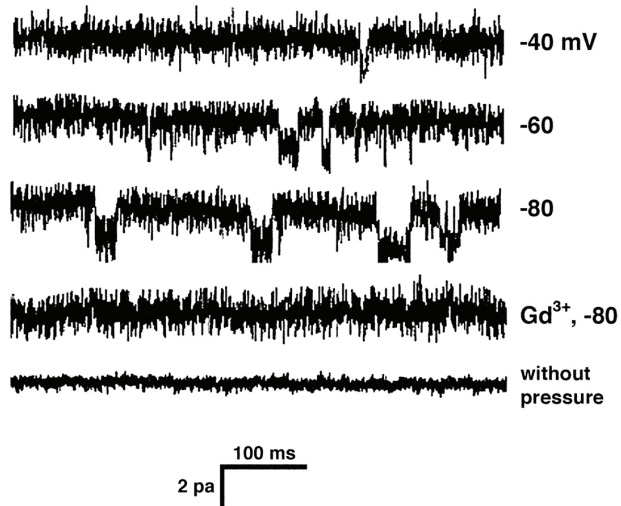
Which is generated by Ca^{2+} influx at the growing tip. The influx is correlated with tip growth rates.



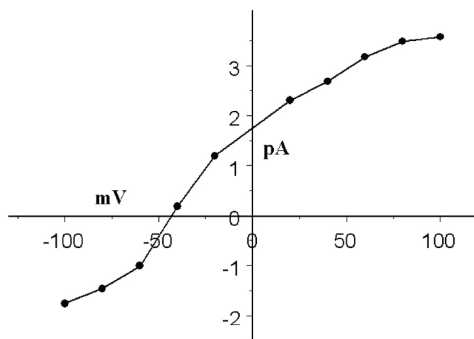
Source: Pierson ES, DD Miller, DA Callaham, J van Aken, G Hackett, PK Hepler (1996) Tip-localized calcium entry fluctuates during pollen tube growth. *Developmental Biology* 174:160–173.

The SA K⁺ channel in pollen protoplasts.

A



B

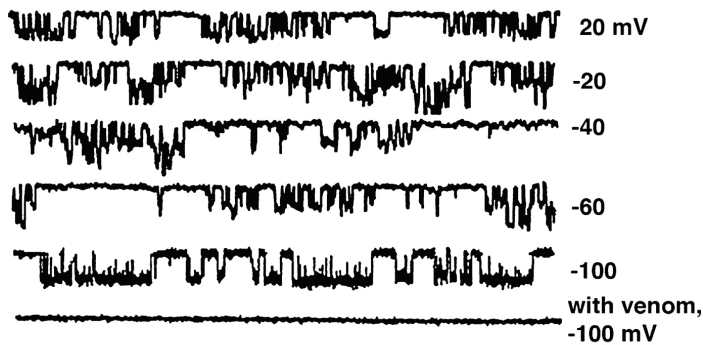


A, Representative sweeps from an outside-out patch containing the SA K⁺ channel. These sweeps are all from the same patch. The first four sweeps were done with -10 kPa pressure applied to the pipette. As the bottom two sweeps show, 10 μM Gd³⁺ or lack of pressure abolished all channel activity. Gd³⁺ took about 10 min to be fully effective, and the trace shown was after recorded slightly more than 10 min after Gd³⁺ addition. B, I-V curve for the channel, compiled from 30 patches.

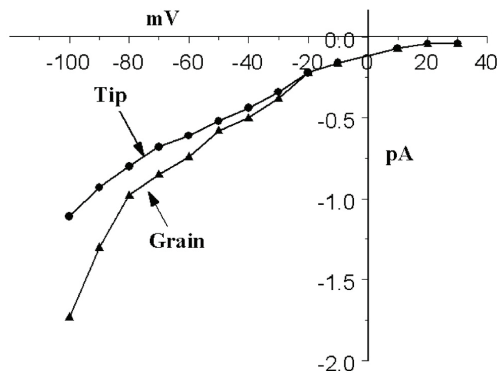
Dutta R, KR Robinson (2004) Identification and characterization of stretch-activated ion channels in pollen protoplasts. *Plant Physiology* 135:1398–1406.

The SA Ca²⁺ channel in pollen protoplasts.

A



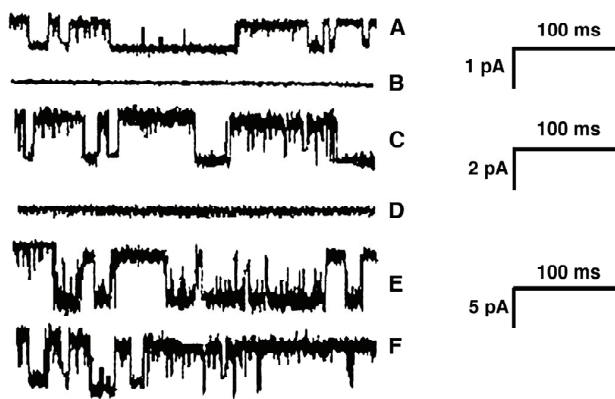
B



A, Sweeps from an outside-out patch containing an SA Ca²⁺ channel. As with the SA K⁺ channel (Fig. 2), no channel activity was detected in the absence of pressure or the presence of 10 μ M Gd³⁺. In some sweeps, two channels could be seen, as well as channel substates. B, The I-V curve for the SA Ca²⁺ channels from 25 patches. The curves are approximately linear for negative holding potentials. Also included here are the data from patches pulled from tip protoplasts (see text and Fig. 4).

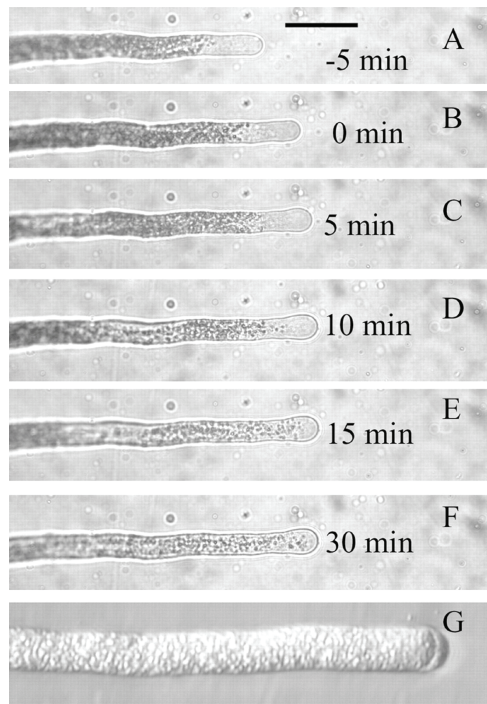
Dutta R, KR Robinson (2004) Identification and characterization of stretch-activated ion channels in pollen protoplasts. *Plant Physiology* 135:1398–1406.

The effect of spider venom at a dilution of 3,000 on pollen protoplast channels.



All sweeps at -100 mV. **A, C, and E** show channel opening of the SA Ca^{2+} channel, the SA K^{+} channel, and the spontaneous K^{+} channel, respectively. **B, D, and F** show the effects of venom on these channels. The venom abolishes activity of two SA channels (**B and D**) but has no effect on the spontaneous channel (**F**). The current scale bar represents 1 pA for A and B, 2 pA for C and D, and 5 pA for E and F.

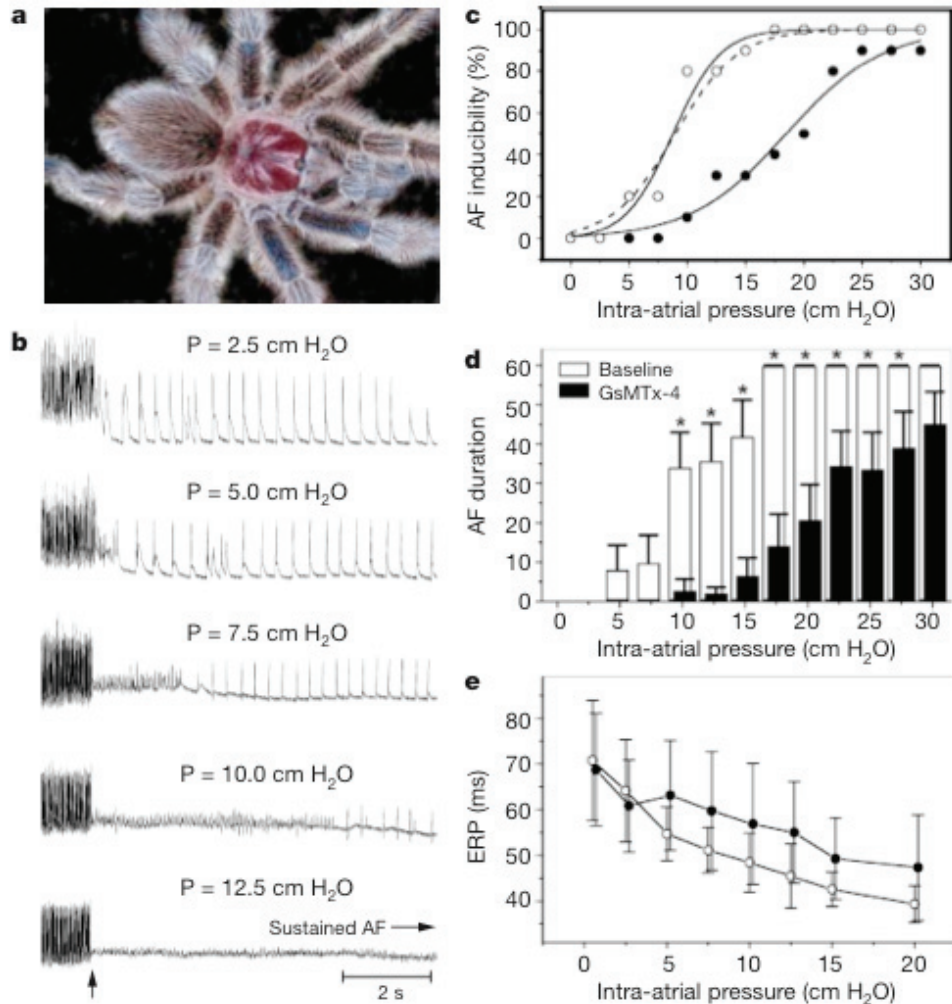
Effect of spider venom at a dilution of 3,000 on pollen tube growth.



A to F, Successive photographs of a pollen tube taken at the indicated time with respect to the time of addition of venom, which was just after the photograph in **B** was taken. Pollen tubes were embedded in a thin layer of agarose, which is covered with medium, so small molecules take a few minutes to diffuse to the tubes after they are added to the medium. Growth slows within 5 min and ceases by 10 min after venom addition, and some swelling of the tip is evident. Scale bar for A to F = $50\ \mu\text{m}$. **G**, A different tube at higher magnification, 30 min after venom addition. The plasmolysis at the tip and the complete loss of the clear zone are typical results of treatment with venom.

Dutta R, KR Robinson (2004) Identification and characterization of stretch-activated ion channels in pollen protoplasts. *Plant Physiology* 135:1398–1406.

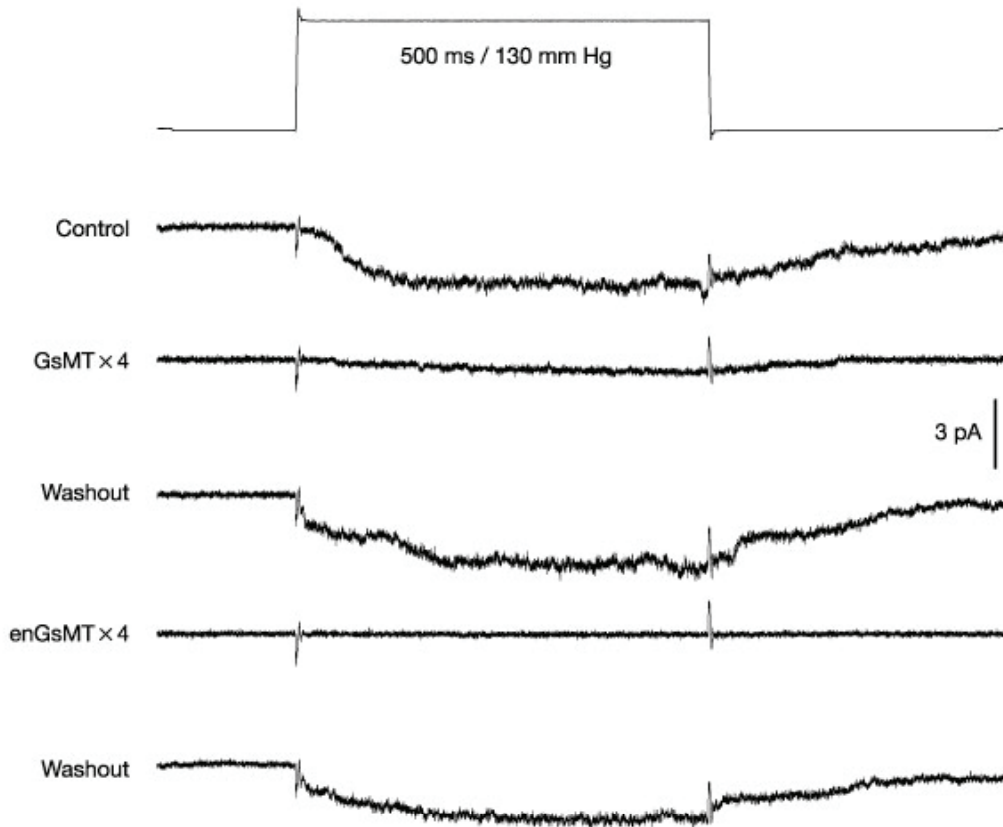
Inhibition of atrial fibrillation by GsMtx-4 during stretch.



a, The spider *Grammostola spatulata*, whose venom is the source of the inhibitory peptide. **b**, Bipolar atrial electrograms showing an increase in atrial fibrillation (AF) with pressure, becoming sustained at 12.5 cm H₂O. The probability of inducing AF was increased by stimulating the heart with a short burst of high-frequency pacing before each measurement (arrow). **c**, Induction of AF lasting more than 2 s: circles, control; filled circles, in the presence of 170 nM GsMtx-4. Dashed line indicates the response after 20-min washout. **d**, Duration of AF (n=7) as a function of pressure (mean ± SE). GsMtx-4 (170 μM) decreased the average time to spontaneous recovery from AF (asterisks, P<0.05). **e**, GsMtx-4 did not block stretch-induced shortening of the refractory period (n=10).

Bode F, F Sachs, MR Franz (2001) Tarantula peptide inhibits atrial fibrillation. *Nature* 409:35–36.

The averaged current from a rat astrocyte outside-out patch is inhibited by both GsMTx4 and enantiomer enGsMTx4 (5 μM)³.

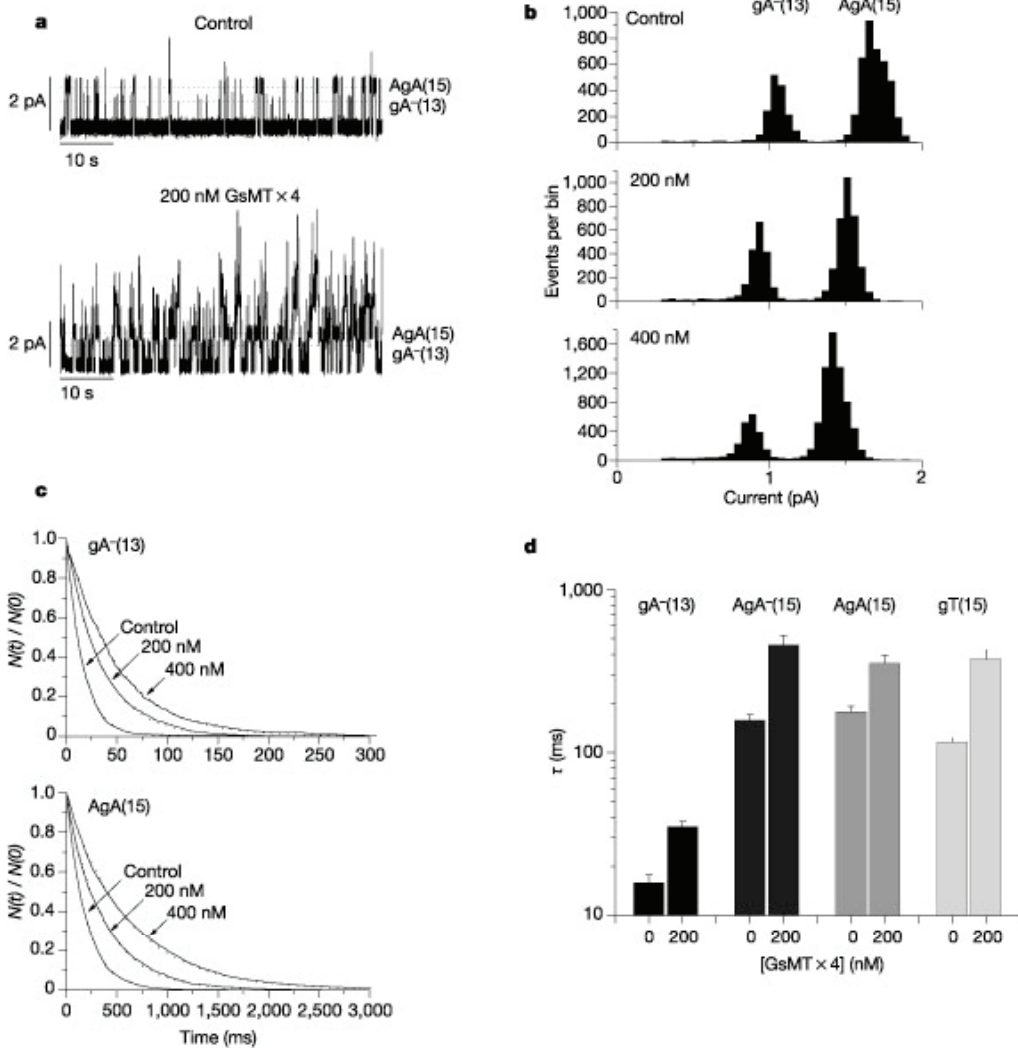


This implies that the inhibition cannot be caused by a specific binding site on the channel, since an enantiomer cannot bind to the same site as the 'anti-enantiomer'. Indeed, given that the spider venom inhibits many mechanosensitive channels from diverse organisms *trans-Kingdom*, a specific binding site is unlikely. Another mechanism of inhibition must exist.

Bilayer-dependent inhibition of mechanosensitive channels by neuroactive peptide enantiomers. By TM Suchyna, SE Tape, RE Koeppel II, OS Andersen, F Sachs, PA Gottlieb. *Nature* 430, 235-240 (8 Jul 2004)

³ "To examine whether GsMTx4 could alter SAC function through a purely bilayer-dependent mechanism, we synthesized enGsMTx4 from d amino acids, and tested its effect on SACs. Except for its optical properties, enGsMTx4 is indistinguishable from wild-type GsMTx4. Surprisingly, enGsMTx4 inhibits SACs with similar efficacy to GsMTx4 (Fig. 3). Thus, GsMTx4 is unlikely to alter SAC gating by a lock-and-key mechanism..."

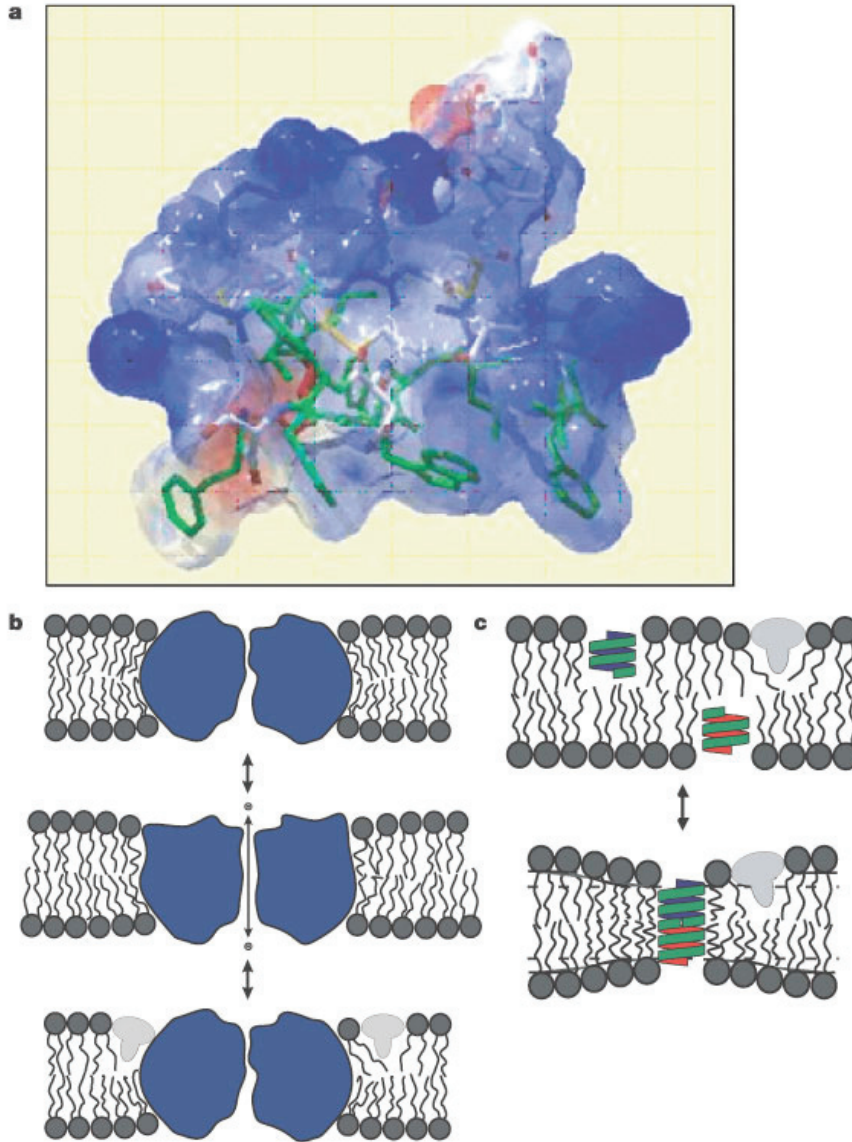
Spider Venom Stimulates Gramicidin Channel Activity



a, Current traces before and after addition of 200 nM GsMTx4 to both sides of a bilayer doped with chain-shortened des-Val 1-Gly 2-gA ($gA^{-}(13)$) and [Ala 1]gA ($AgA(15)$) (numbers in parentheses denote number of residues in the sequence): gA^{-} is the enantiomer of gA20. **b**, **c**, Single-channel currents are reduced (**b**) and lifetimes increased (**c**) as a function of GsMTx4 concentration (see Methods). **d**, Average lifetime (τ) as a function of channel length, helix sense and identity of the aromatic residues at the channel/solution interface. $gA^{-}(13)$ and $AgA(15)$ as above, $AgA^{-}(15)$ is [D-Ala 1]gA-, gT is [Tyr^{9,11,13,15}]gA (ref. 21). 200 nM GsMTx4; columns and error bars denote mean \pm s.d. (n greater than or equal to 3); 100 mV applied potential.

Bilayer-dependent inhibition of mechanosensitive channels by neuroactive peptide enantiomers. By TM Suchyna, SE Tape, RE Koeppel II, OS Andersen, F Sachs, PA Gottlieb. Nature 430, 235-240 (8 Jul 2004)

Spider Venom: Proposed Mode of Inhibition



a, Rendered image of GsMTx4 coloured by Coulomb electrostatic potential at $2.8 \text{ kBT}/e$ (k_B is the Boltzmann constant, T temperature in K and e the elementary charge). Positive residues (blue); negative residues (red); hydrophobic residues (green). **b**, Schematic diagram of how GsMTx4 may inhibit SACs by perturbing the channel/bilayer boundary without necessarily being in physical contact with the channel. **c**, Schematic diagram of gramicidin A channel formation, which involves a local bilayer thinning. The bilayer deformation energy could be reduced if GsMTx4 were near/at the channel, which would increase the dimerization constant (channel activity).

Bilayer-dependent inhibition of mechanosensitive channels by neuroactive peptide enantiomers. By TM Suchyna, SE Tape, RE Koeppel II, OS Andersen, F Sachs, PA Gottlieb. *Nature* 430, 235-240 (8 Jul 2004)

doi:10.1016/j.bpj.2010.09.022 | How to Cite or Link Using DOI
Copyright © 2010 Biophysical Society Published by Elsevier Inc.
Permissions & Reprints

Article

Effects of GsMTx4 on Bacterial Mechanosensitive Channels in Inside-Out Patches from Giant Spheroplasts

Kishore Kamaraju[†], Philip A. Gottlieb[‡], Frederick Sachs[‡], and Sergei Sukharev[†]

[†] Department of Biology, University of Maryland, College Park, Maryland

[‡] Department of Physiology and Biophysics, Center for Single Molecule Biophysics, State University of New York at Buffalo, Buffalo, New York

Received 30 April 2010; accepted 13 September 2010. Editor: Kenton J. Swartz. Available online 2 November 2010.

Abstract

GsMTx4 is a 34-residue peptide isolated from the tarantula *Grammostola spatulata* folded into an inhibitory cysteine knot and it selectively affects gating of some mechanosensitive channels. Here we report the effects of cytoplasmic GsMTx4 on the two bacterial channels, MscS and MscL, in giant *Escherichia coli* spheroplasts. In excised inside-out patches, GsMTx4 sensitized both channels to tension by increasing the opening rate and decreasing the closing rate. With ascending and descending pressure ramps, GsMTx4 increased the gating hysteresis for MscS, a consequence of slower gating kinetics. Quantitative kinetic analysis of the primary C \leftrightarrow O transition showed that the hysteresis is a result of the decreased closing rate. The gating barrier location relative to the open state energy well was unaffected by GsMTx4. A reconstructed energy profile suggests that the peptide prestresses the resting state of MscS, lowering the net barrier to opening and stabilizes the open conformation by ~ 8 kT. In excised patches, both MscL and MscS exhibit reversible adaptation, a process separable from inactivation for MscS. GsMTx4 decreased the rate of reversible adaptation for both channels and the MscS recovery rate from the inactivation. These measurements support a mechanism where GsMTx4 binds to the lipid interface of the channel, increasing the local stress that is sensed by the channels and stabilizing the expanded conformations.

